CDF/DOC/TRIGGER/CDFR/5485
17th November 2000
Version 1.0

A Run II Soft Lepton Tag – based Trigger for $H^0 + V$

P. Azzi, A. Castro, M. P. Giordani, P. Maksimovič, L. Scodellaro

Abstract

In this note we present a proposal for a Run II multijet trigger aimed at selecting H^0+Z^0/$W^{\pm}\rightarrow$ *had* events via a tagging of the soft leptons produced in the semileptonic decays of b or c quarks. This tool is meant to be efficient for Higgs masses up to $\sim$130 GeV/c^2, where $H^0\rightarrow b\bar{b}$ is the dominant decay process.

1 Motivations

One of the primary goals for Run II at TEVATRON is the search for Higgs bosons. Studies based on Run II simulations show that, for an integrated (CDF and D0) luminosity of the order of 10 fb^{-1}, a 3σ H^0 evidence is at reach for $m_H \lesssim 130$ GeV/c^2, while a 95% C.L. exclusion is achievable for $m_H \lesssim 190$ GeV/c^2 [1].

Although Higgs production at TEVATRON is dominated by gluon fusion ($\sigma \sim 1$ pb for m_H=130 GeV/c^2), its associated production with a vector boson is a much more promising channel despite its lower cross-section ($\sigma \sim 0.1$ pb for m_H=130 GeV/c^2 – see fig. 1), since it allows a much more effective control of the QCD background by the vector boson reconstruction.

For $m_H \lesssim 130$ GeV/c^2, the favoured Higgs decay channel proceeds through $b\bar{b}$ production (*B.R.* $\sim$70% – see fig. 1), which makes b-jet identification a crucial feature. Experimentally, two approaches can be pursued: the first one – object of this study – consists of tagging the soft leptons produced by the semileptonic decay of the B-hadrons and is complemental with the second one, which on the other hand exploits the large B-hadron lifetime. The latter procedure implies the search for secondary vertices, therefore requiring a vertex detector.

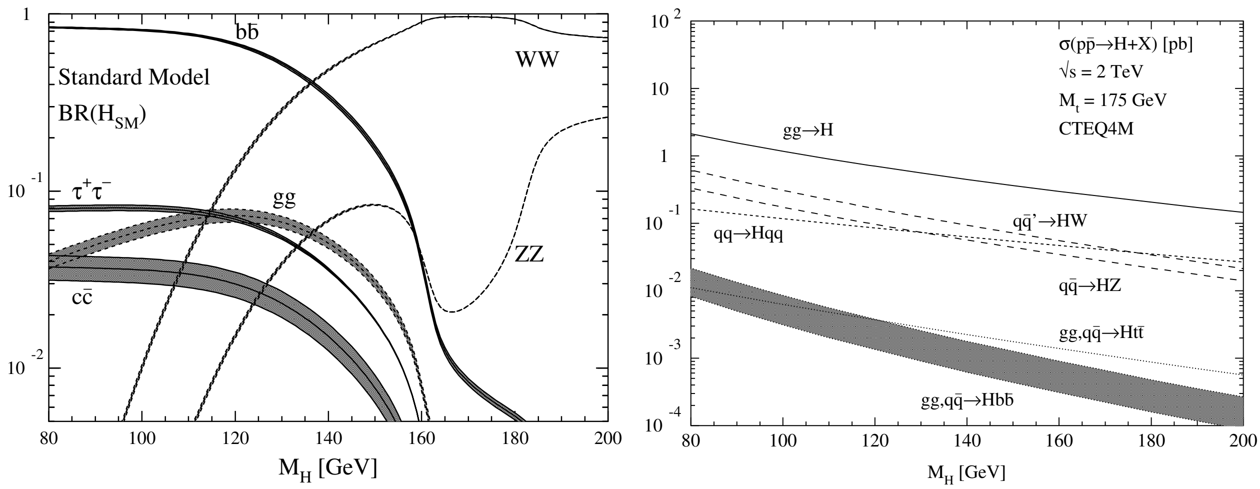

Figure 1: *SM Higgs branching ratios (left) and production cross-section at* TEVATRON *(right) in terms of* m_{H}.

2 Run I trigger

The design goal of the Run I multijet trigger was the search for the top quark [2], which eventually culminated with its discovery [3]. The essential requirements of this trigger in Run Ib were[1]:

LEVEL 2: $\Sigma E_T \geqslant 120\,\mathrm{GeV}$, $\Sigma E_T^{cl} \geqslant 125\,\mathrm{GeV}$, $N_{cl} \geqslant 4$ $(E_T^{cl} \geqslant 15\,\mathrm{GeV})$

LEVEL 3: $N_{jet}^{0.4} \geqslant 4$ or $N_{jet}^{0.7} \geqslant 4$ $(E_T^{jet} \geqslant 10\,\mathrm{GeV})$

The data sample collected with this trigger was also used in a subsequent search for the Standard Model Higgs boson [4]. However, given the fact that the multijet trigger criteria were motivated by the kinematics of the top quark decay into six jets, the trigger was found to be rather inefficient for the Higgs search. Our goal is to improve this condition by loosening the kinematics cuts while reducing the trigger rate by some other means, for example by tagging the soft leptons produced in the semileptonic decay of b and c quarks originated by the bosons.

[1]In the following, the symbols ΣE_T and ΣE_T^{cl} stand for the sums over calorimetry towers and Level 2 clusters E_T respectively.

3 Data samples

For the simulation of Run II variables (both for Monte Carlo and data samples), the Run I software package together with the RUN2TRS simulation has been used.

Signal A sample of $\sim$10000 $\mathrm{H}^0+\mathrm{Z}^0/\mathrm{W}^\pm \to \mathrm{b}\overline{\mathrm{b}}+\mathrm{q}'\overline{\mathrm{q}}$ events (m_{H}=120 GeV/c^2) have been generated at $\sqrt{s}=2$ TeV with PYTHIA and subsequently processed through the QFL simulator.

Background Level 2 & 3 trigger background rate estimates have been performed on a sample of $\sim$60000 JET20 events collected during Run Ib [2].

Further samples of $\sim$ 30000 conversion electrons and $\sim$ 10000 muons from $\mathrm{J}/\psi(1\mathrm{S})$ decay, collected in the Run Ib with the CEM_8_CFT_7_5_XCES and PSIA_DIMUON_JPSI_SINGLE_V1 triggers respectively, have been used in order to determine the efficiencies of lepton requirements.

In the following, the implicit assumption of a medium luminosity scenario for Run II has been made; therefore, the value $\mathcal{L}=10^{32}\,\mathrm{cm}^{-2}\mathrm{s}^{-1}$ has been supposed in all rate estimations.

4 Level 1

4.1 Calorimetry

The Level 1 calorimetric primitive has been taken from the QCD inclusive jet path, which requires at least one trigger-tower with energy content above a certain E_T threshold. Two threshold values have been so far proposed (5 and 10 GeV), but only the highest one will be used in the definition of an unprescaled Level 1 primitive [5], which hereafter will be considered for our study.

The signal efficiency after the requirement of an inclusive trigger-tower with $E_T \geqslant 10$ GeV is $\gtrsim$98%, while the rate[3] is 2.7 kHz (for $\mathcal{L}=10^{32}\,\mathrm{cm}^{-2}\mathrm{s}^{-1}$).

[2] Since it has soon been apparent that almost the totality ($\sim$ 99%) of the signal events passes the Run I JET20 trigger.

[3] See [5], § 3.2.

5 Level 2

5.1 Calorimetry

As previously mentioned (see § 2), the Run I multijet trigger was not optimized for Higgs searches and, consequently, was found to be rather inefficient in selecting $H^0+Z^0/W^{\pm}$ events (see also [6] and references cited therein). Fig. 2 shows the Run I multijet requirements on ΣE_T^{cl} and on the number of clusters at Level 2.

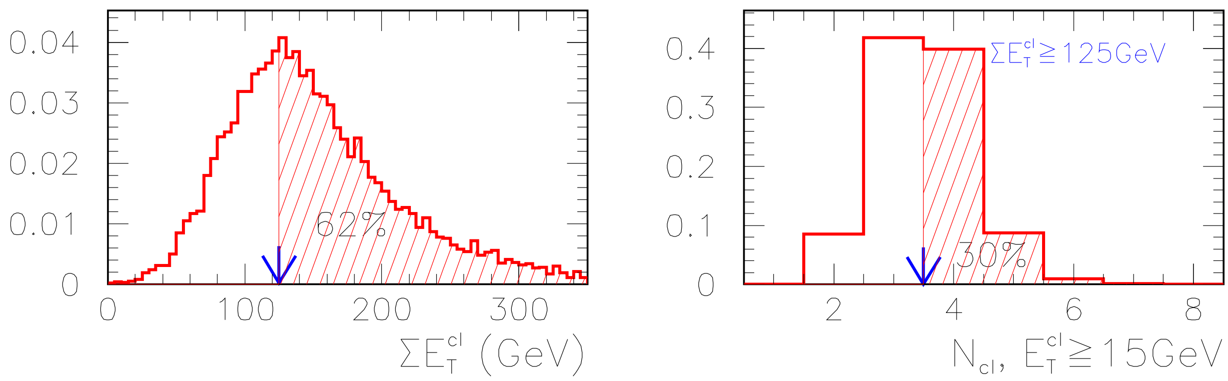

Figure 2: *Level 2 signal distributions: ΣE_T^{cl} and number of clusters ($E_T^{cl} \geqslant 15$ GeV).*

Our initial modification towards an Higgs-optimized multijet trigger has been motivated by topological considerations on the signal: $H^0+Z^0/W^{\pm} \rightarrow$ *had* events are expected[4] to produce four jets in the final state; taking into account the eventuality of loosing one jet or merging two of them, the possibility of requiring only three clusters at Level 2 has been considered, which, according to fig. 2 (right plot), would guarantee a significant increase in the efficiency.

At this point, two parameters still need to be fixed: the E_T threshold of the (at least) three clusters and the ΣE_T threshold. The possibility of requiring unequal thresholds for the cluster E_T has been investigated, but led to no significant improvement in the signal to background ratio; the reason for this can be found in the topology of the main background (QCD 3-jet production), in which the third jet is radiated by one of the leading ones [9].

A further step towards a signal to background ratio enhancement can be pursued by constructing an optimal ΣE_T^{cl} primitive; in principle, ΣE_T^{cl} could be defined as the sum of the E_T of all *'jet'* clusters (3 GeV seed and 1 GeV shoulder threshold on both hadronic and e.m. energies) with energy content above a certain threshold. In the following we consider

[4] Disregarding initial and final state radiation processes at this time.

only two cases, one where the sum is extended to all clusters ($E_T^{min} = 3\,\mathrm{GeV}$) and the other one (indicated by $\Sigma E_T 10$) where only clusters with $E_T \geqslant 10\,\mathrm{GeV}$ are considered, which represent some kind of 'extreme cases'.

In order to take into account the natural correlation between the ΣE_T and the number of clusters, the behaviour of different combinations of ΣE_T primitives and cluster E_T thresholds has been studied; the results are shown in fig. 3.

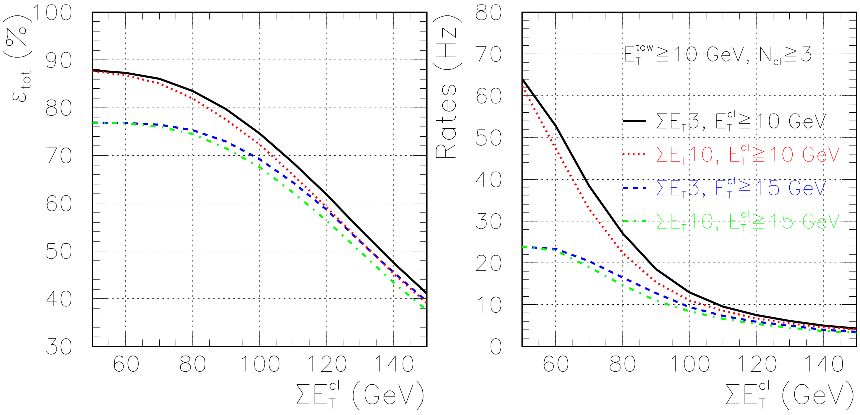

Figure 3: *Level 2 efficiencies (left) and rates (right) for different calorimetric cuts plotted as functions of the corresponding* ΣE_T *primitives.*

The choice of the optimal Level 2 primitive is performed on the basis of efficiency maximization; momentarily disregarding any further selections at Level 2 (see § 5.2), this procedure, being limited by a bandwidth constrain, is affected by the typology of the subsequent Level 3 selection. Since no secondary vertex explicit reconstruction will be made at Level 3, a rate level of $\sim 15\,\mathrm{Hz}$ is acceptable; therefore, an optimal performance can be pursued with the Level 2 requirement:

$$\Sigma E_T 10 \geqslant 90\,\mathrm{GeV},\ N_{cl}(E_T^{cl} \geqslant 10\,\mathrm{GeV}) \geqslant 3,$$

which correspond to an efficiency of 77.6% and a rate of 15.4 Hz.

A graphical representation of the Level 2 calorimetric selection is shown in fig. 4, where the distributions of the calorimetric quantities at Level 2 for signal and data are compared.

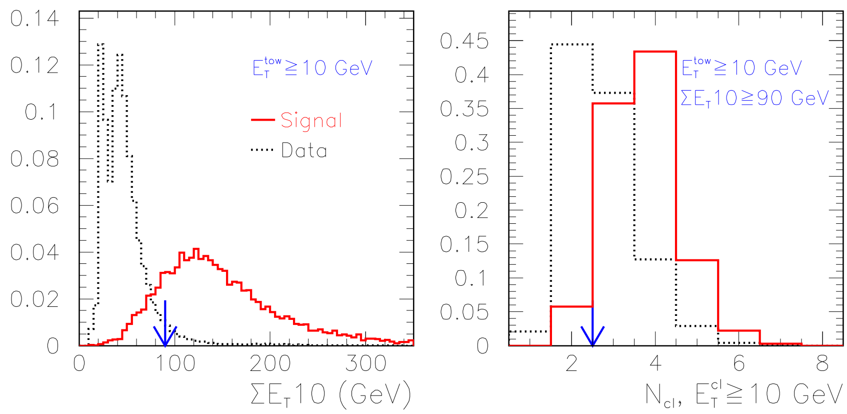

Figure 4: *$\Sigma E_T 10$ (left) and number of clusters with $E_T^{cl} \geqslant 10\,\mathrm{GeV}$ (right) distributions as functions of* $\Sigma E_T 10$.

5.2 Leptons

5.2.1 Electrons

Electrons emerging from the semileptonic decay of B and D-hadrons produced by H^0 and $Z^0/W^\pm$ exhibit a soft p_T spectrum (see fig. 5); Run I single electron triggers, being focused on electrons characterized by higher p_T spectra, cannot be applied. Electrons coming from B and D-hadron decays are not expected to be isolated, which, besides their soft p_T spectrum, makes them difficult to tag by means of their energy deposition in the electromagnetic calorimeter, due to the broad $\eta - \phi$ segmentation ($\Delta\eta \simeq 0.1, \Delta\phi = 15^0$) of its towers. A much finer segmentation in ϕ ($\sim 2^o$) is however offered by the strip chambers (CES), whose information is available at Level 2 as XCES bits; a XCES bit is set for a given XFT track[5] if the sum of the signals collected by the four wires closest to the track extrapolation point at CES exceeds a certain threshold (two

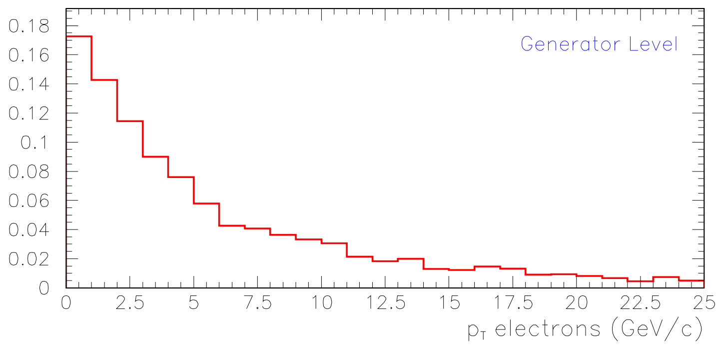

Figure 5: *p_T spectrum for generator level electrons produced in* B *and* D*-hadron decays.*

[5]In order to simulate the XFT behaviour within the Run II environment, the package Run2Trs uses (Run I) smeared CTC tracks for mimicking the XFT output.

thresholds will be available in Run II)[6].

Due to poor CES simulation by QFL, it has been necessary to estimate the XCES efficiency in function of the pulse-height threshold for true electrons from a data sample; the conversion electrons extracted from a sample of events collected in Run Ib with the CEM_8_CFT_7_5_XCES trigger has been used for the purpose. Conversion electrons have been identified by searching for conversion pairs in which the most energetic leg role was played by the trigger electron; once all conversion partner candidates for each trigger electron were found, a constrained fit was applied and the best fit tagged as soft leg [10]. Applying further standard electron cuts[7] to the soft legs has made possible the collection of an unbiased sample to test the CES efficiency with respect to the ADC pulse-height associated to the electron track.

As shown in fig. 6, the selected sample of electrons exhibit a softer p_T spectrum than signal electrons; if on one hand this makes the efficiency evaluation conservative, on the other it may lead to a too conservative estimate, which could invalidate the discriminating power of CES-based requirements. In order to avoid this, two procedures for estimating the CES efficiency have been tested. In one case a simple counting experiment has been performed on the conversion sample irrespective of its p_T spectrum; in the other, the counting experiment has been biased in order to keep track of the shape of the p_T spectrum of signal electrons. The efficiency is then

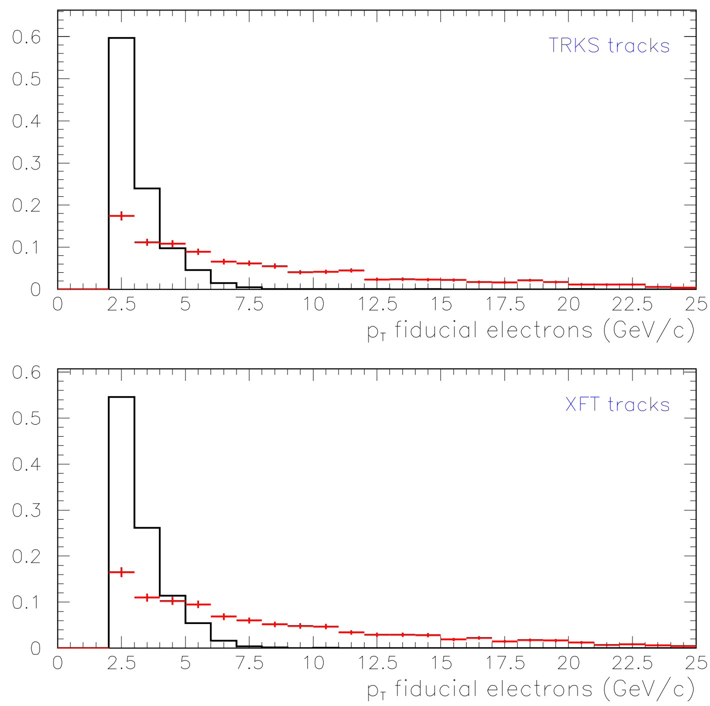

Figure 6: *p_T spectrum for* TRKS *and* XFT*-reconstructed* b *and* c *electrons (crosses) with respect to conversion electrons (solid).*

[6]Considering a single CES wedge (corresponding to $\Delta\phi = 15^o$), the 32 wires aligned along each CES η-segment are clustered in groups of four adjacent wires; the track extrapolation at CES identifies the cluster (*bit*) of wires which are to be summed. Since only azimuthal information is available at Level 2, four bits are associated to a single track; the track XCES bit then is set if at least one of the four bits fulfills the minimum pulse-height requirement (see [7], § 12.4.2).

[7]These cuts obviously do not include any requirement on wire or strip energies recorded by the strip chambers.

estimated by the expression:

$$\epsilon_e = \frac{\sum_{i=1}^{N^p} w_i}{\sum_{i=1}^{N^p+N^f} w_i} \ , \tag{1}$$

where N^p and N^f are the number of electrons respectively passing and failing the XCES requirement; each electron has been weighted according to its p_T by a factor w_i, whose values have been calculated from the ratio of signal to conversion electrons (normalized) p_T spectra[8]. In the case of unweighted procedure, expression (1) trivially reduces to:

$$\epsilon_e = \frac{N^p}{N^p + N^f} \ . \tag{2}$$

The results of both procedures, with the 90%-efficiency limit highlighted, are shown in fig. 7.

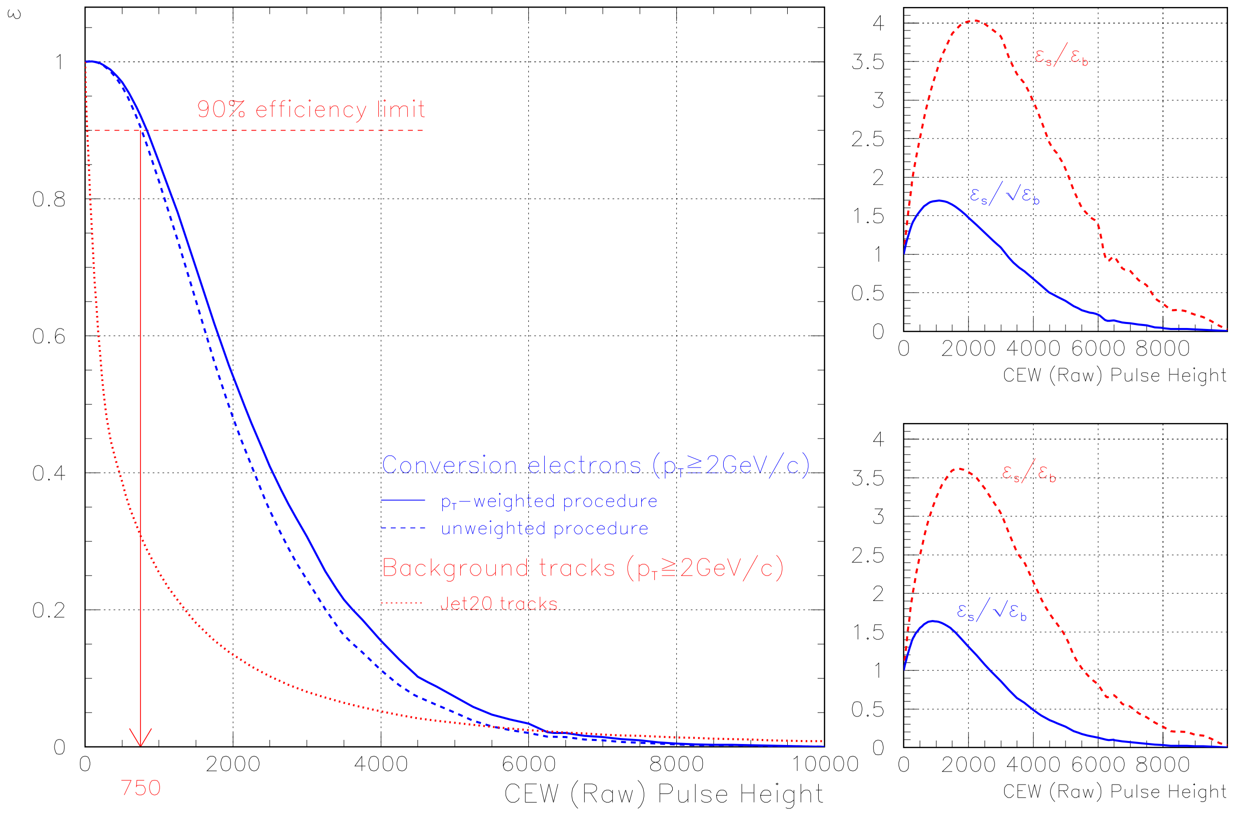

Figure 7: *Left:* CES *efficiency vs. minimum* XCES ADC *pulse-height threshold for conversion soft leg electrons and for generic background tracks* ($p_T \geqslant 2\,\mathrm{GeV/c}$). *Right: S/B gain (dashed) and significance (solid) for weighted (upper) and unweighted (lower) procedures.*

[8] More suitably binned distributions have been used rather than the ones depicted in fig. 6.

The two procedures lead to comparable results; in particular, in both cases, the same threshold value of 1000 ADC counts has been found on the basis of significance maximization (see solid curves in left plots of fig. 7). The efficiency for the corresponding XCES requirement (see solid and dashed curves in right plot of fig. 7) are 85.4% and 82.6% for the weighted and unweighted procedures respectively[9].

The suitability of the unbiased sample, with particular reference to the p_T spectrum being softer than expected for signal electrons, has been tested by studying the p_T dependence of the XCES requirement which is under study; fig. 8, which has been obtained by means of expression (2), shows that a plateau value is reached already at $p_T \simeq 5\,\mathrm{GeV/c}$. For this reason, one can assume that the modeling of the efficiency curve can be safely estabilished using the soft electron sample, without requiring further statistics at higher p_T.

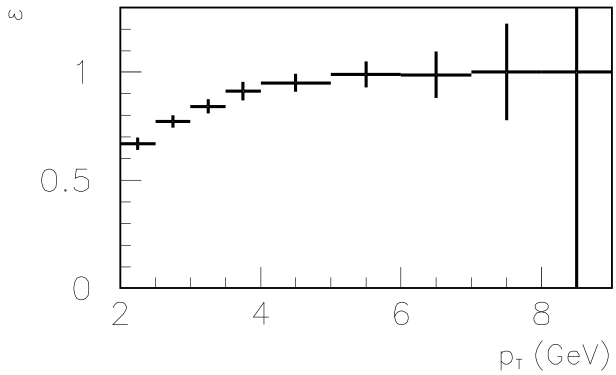

Figure 8: *p_T dependence of* XCES *requirement as estimated on conversion electrons (overflow bin for $p_T \geqslant 8\,\mathrm{GeV/c}$).*

Hence, the poor CES simulation has been by-passed by weighting each generated electron associated to a XFT track with transverse momentum $p_T(\geqslant 2\,\mathrm{GeV/c})$ extrapolating to the CES fiducial volume by the corresponding efficiency $\epsilon_e(p_T)$.

Finally, the so calculated efficiency per electron leads to the efficiency[10] for selecting a 'signal' event, by this meaning an event containing a CES-fiducial electron (with $p_T \geqslant 2\,\mathrm{GeV/c}$) produced in the semileptonic decay of a B or D-hadron coming from V or H^0; this is simply given by the formula:

$$P_{evt} = 1 - \prod \left(1 - \epsilon_e(p_T)\right) \ , \tag{3}$$

where the product is extended over all generated electrons fulfilling the above requirements in a given event.

Contributions to the rate, on the other hand, come from those background events which contain at least one XFT track with $p_T \geqslant 2\,\mathrm{GeV/c}$ associated to a XCES pulse-height of at least 750 ADC counts. Results of the selection are summarized in fig. 9.

[9]Note that a 90% efficiency is achieved by the unweighted procedure for a pulse-height threshold of 750 ADC counts, which is in agreement with the estimations quoted in [7] (fig. 4 and tab. 4 on pag. 13) and [8] (fig. 5 on pag. 10).

[10]Efficiencies will here be defined with respect to generated events and not to 'analizable' ones.

The magnitude of the efficiency drop in passing from the solid curve (Level 2 calorimetry only) to the dotted one (XCES pulse-height requirement added) and the rate behaviour can be interpreted as follows. On one hand, the efficiency drop can be explained considering that in only 30.0% of the events in which a signal electron has been produced, a signal electron with $P_T \geqslant 2\,\mathrm{GeV/c}$ is emitted within the CES acceptance (after calorimetric requirements, with $\Sigma E_T 10 \geqslant 90\,\mathrm{GeV}$). On the other hand, the small rate rejection can be interpreted in terms of fake tags. In other words, particles which are either non-signal[11] electrons or non-electrons fulfilling the XCES pulse-height requirement – which are not taken into account in the computation of the efficiency – can contribute significantly to the rate, being implicitly included in its definition.

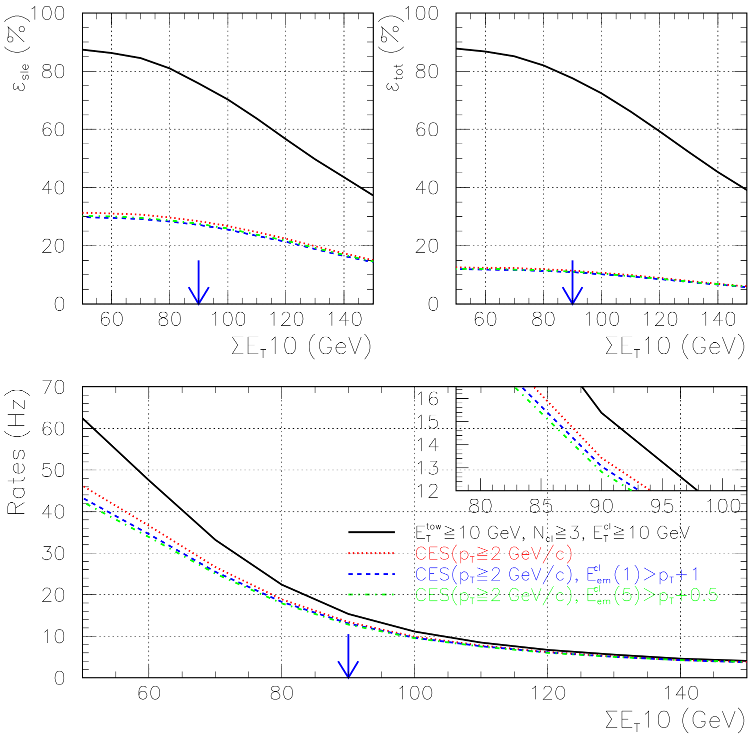

Figure 9: *Level 2 efficiency in events with at least one 'signal' electron (upper left), in* $H^0 + Z^0/W^{\pm} \rightarrow$ *had events (upper right)and rate (below) in terms of* $\Sigma E_T 10$.

The effective significance of this hypothesis can be tested evaluating a fake tag probability defined as the probability for a CES-fiducial track of passing the XCES pulse-height requirement; this can be done directly on the JET20 events, assuming there is no significant enrichment in heavy flavours in the sample (see fig. 10).

[11] I.e. not produced in the semileptonic decay of a b ore c quark associated to a boson.

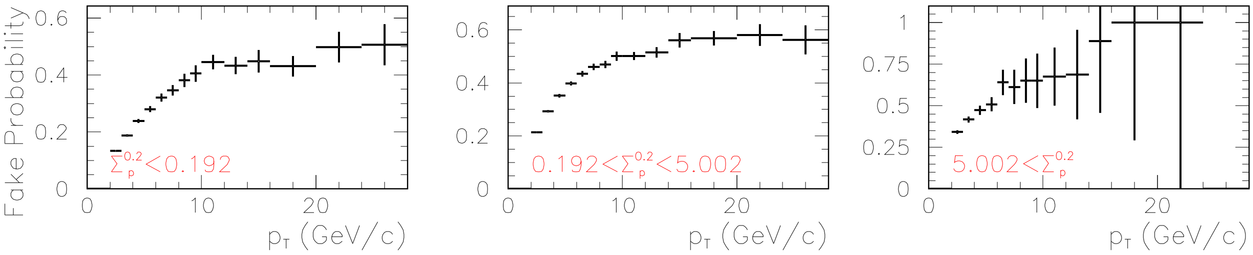

Figure 10: *Fake tag probability as a function of track p_T for different isolation ranges.*

The fake tag probability is expected to depend essentially on two variables: the track p_T and its isolation, which has been parametrized[12] according to [12]. Each track associated to a non-null fake tag probability will therefore result in an enhancement in the P_{evt}, according to a simple generalization of expression (3). The magnitude of the fake probability (shown in fig. 10) and, consequently, the behaviour of the solid and dotted curves for efficiency and rate shown in fig. 11, appears to agree with the hypothesis made; this, furthermore, implies that the XCES pulse-height requirement on its own is not a suitable selection for signal events.

A more strict selection on 'signal' electrons can be pursued at Level 2 by matching (in ϕ only) the XFT-tracks with electromagnetic clusters in the CEM; for this purpose, two different procedures have been considered: the first one uses low p_T electron clusters (seed 3 GeV, shoulder 2.5 GeV– known as 'type 1'), while for the second

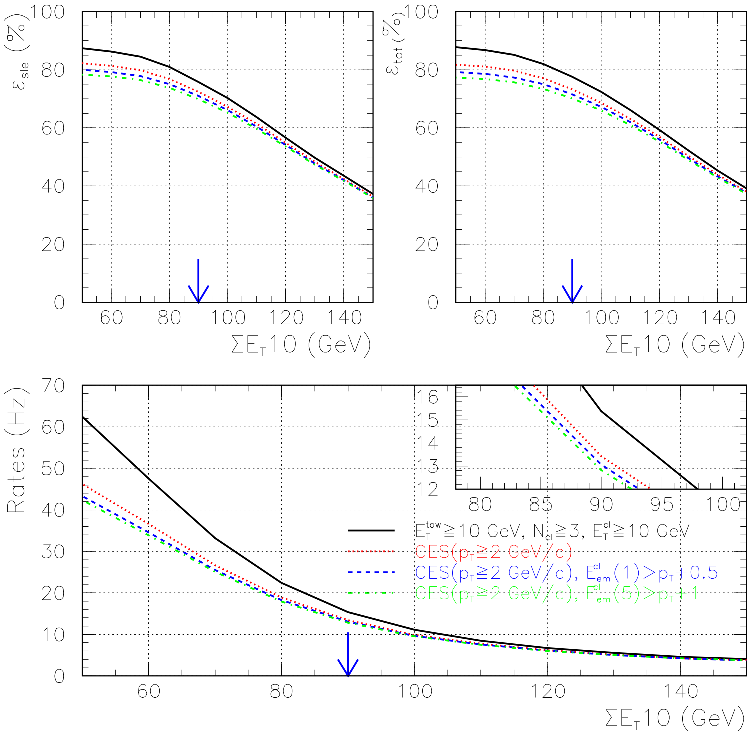

Figure 11: *Level 2 efficiency in events with at least one 'signal' electron (upper left), in* $H^0+Z^0/W^\pm \to$ *had events (upper right) and rate (below) in terms of* $\Sigma E_T 10$ *when fake electrons contribution is taken into account.*

[12]Track isolation is estimated by the quantity $\Sigma_p^{0.2}$, which is defined as the sum of the momenta of all tracks contained in a cone with $r_{\eta\phi}=0.2$ around the considered track.

one a new type of e.m. clusters has been hypotized (seed[13] 2.5 GeV, infinite shoulder – later referred as 'type 5'). Both procedures are then added to the XCES pulse-height requirement; their effect on both efficiency and rates has already been shown in figs. 9 and 11 (see dashed curves) and are reported in table 1.

Selection	**Efficiency**		**Rate**
		+fakes	(JET20)
Calorimetry only	75.8% (77.6%)		15.4 Hz
$p_T(\mathrm{e}) \geqslant 2\,\mathrm{GeV/c}$, $E_{ph} > 1000$	28.4% (11.4%)	72.3% (73.2%)	13.4 Hz
$p_T(\mathrm{e}) \geqslant 2\,\mathrm{GeV/c}$, $E_{ph} > 1000$ (type 1)	27.1% (10.8%)	70.9% (71.5%)	13.1 Hz
$p_T(\mathrm{e}) \geqslant 2\,\mathrm{GeV/c}$, $E_{ph} > 1000$ (type 5)	27.6% (11.0%)	69.9% (70.1%)	12.8 Hz

Table 1: *Level 2 event efficiencies and rate for* $\Sigma E_T 10 \geqslant 90\,\mathrm{GeV}$ *(efficiencies are computed with respect to the total number of events in which a signal electron has been produced – efficiencies on* $\mathrm{H}^0{+}\mathrm{Z}^0/\mathrm{W}^{\pm}{\rightarrow}$ *had are indicated in brackets).*

The introduction of the matching requirements has not supplied a solution to the efficiency drop, which is still much more consistent than the one observed correspondingly in the rate; therefore any further requirement, besides the purely calorimetric ones, is not justified.

5.2.2 Muons

Muon identification essentially works on the basis of a matching between a track and a cluster of hits (*'stub'*) collected in some muon chamber. At Level 2, when only ϕ-matching is possible between stubs and XFT tracks, Run II muon triggers will take advantage of a finer azimuthal resolution[14] (1.25°) than in Run I (when the resolution was 5°). This procedure is simulated by the RUN2TRS package, which uses Run I CTC smeared tracks for mimicking the XFT output and Run I low p_T (3.3 GeV/c) trigger stubs information available at Level 1 for muon chambers performance.

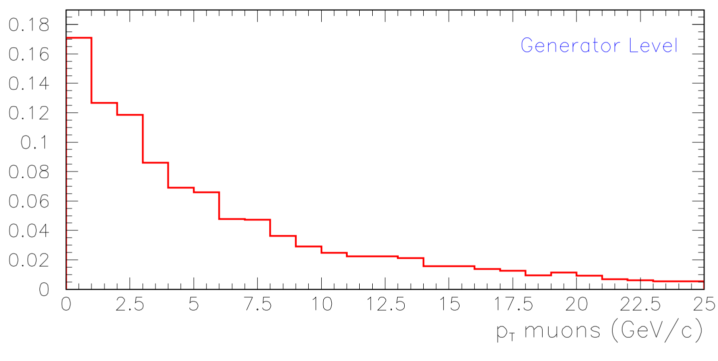

Figure 12: *p_T spectrum for generator level muons produced in* B *and* D*-hadron decays.*

[13]The seed value has been chosen in order to maximize the $S/\sqrt{B}$ ratio, while the shoulder has been set in order to force single-tower clusters, which exploits the highest possible CEM granularity available at Level 2 needed to extract the signal of non-isolated electrons.

[14]This is due to the improved track finder procedure implemented for Run II.

Since, as for electrons, the muons generated in the decay of B and D-hadrons are characterized by a soft spectrum (see fig. 12), the Run II Level 2 trigger efficiencies have been determined on real muons identified in a sample of events collected in Run Ib with the PSIA_DIMUON_JPSI_SINGLE_V1 trigger; in particular, the single muon trigger paths have been considered, which require a Level 1 stub with $p_T \geqslant 6$ GeV/c (CMU, CMP) or $p_T \geqslant 10$ GeV/c (CMX) and at Level 2 a XFT track with $p_T \geqslant 7.5$ GeV/c or $p_T \geqslant 12$ GeV/c matched respectively to a CMU, CMP or CMX reconstructed stub.

Before proceeding in the measurement of the Level 2 muon requirement, consisting of a matching between a low p_T stub and a XFT track, it has been necessary to introduce an unbiased sample of muons. This has been done tagging as 'unbiased' the muon[15] that, for each event, has provided the best vertex-constrained fit to the J/ψ(1S) with the trigger muon. Once the unbiased sample has been determined, and the invariant masses of each 'unbiased μ' – 'trigger μ' pair recorded, two mass regions have been defined: a 3σ window around the J/ψ(1S) peak for the signal and a $4 \div 8\sigma$ region away from the J/ψ(1S) peak for background. Finally, the Run II trigger performance has been tested by means of a counting experiment and its efficiency estimated by the expression (that has to be considered function of the muon p_T):

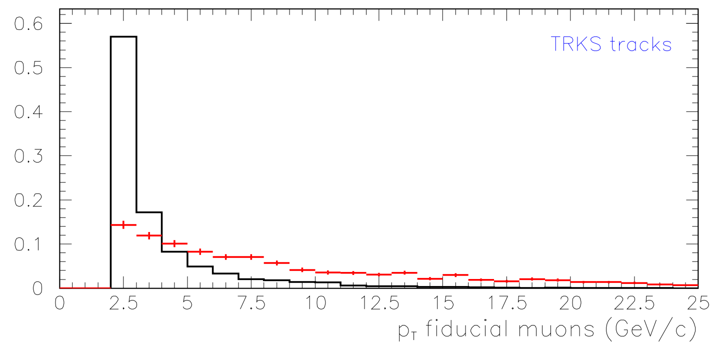

Figure 13: *p_T spectrum for* TRKS*-reconstructed* b *and* c *muons (crosses) with respect to* J/ψ(1S) *muons (solid).*

$$\epsilon_\mu = \frac{N^p_{J/\psi} - N^p_{bgd}}{\left(N^p_{J/\psi} - N^p_{bgd}\right) + \left(N^f_{J/\psi} - N^f_{bgd}\right)} \,, \tag{4}$$

where $N_{J/\psi}$ and N_{bgd} are the number of muons associated to the signal and background mass windows, while the apices p and f indicate passing or failing the Run II trigger requirements.

[15]Defined as a TRKS track with CMU or CMX information.

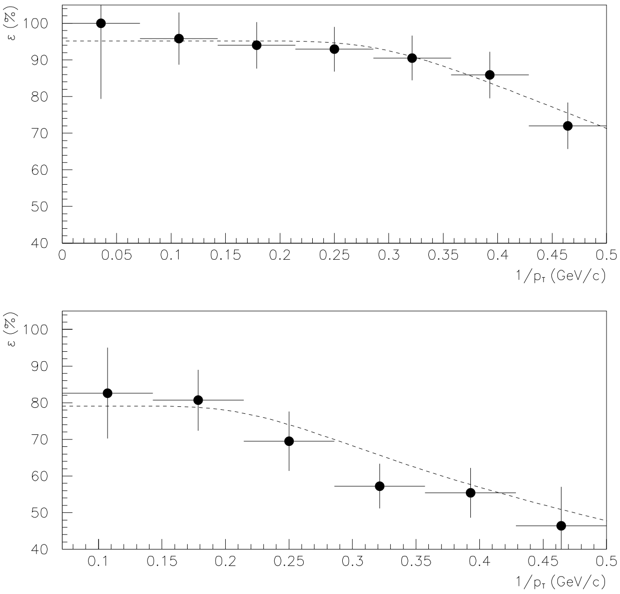

Figure 14: *Run I Level 1 low p_T muon trigger efficiency in terms of $1/p_T$ threshold (top for* CMU *and bottom for* CMX*).*

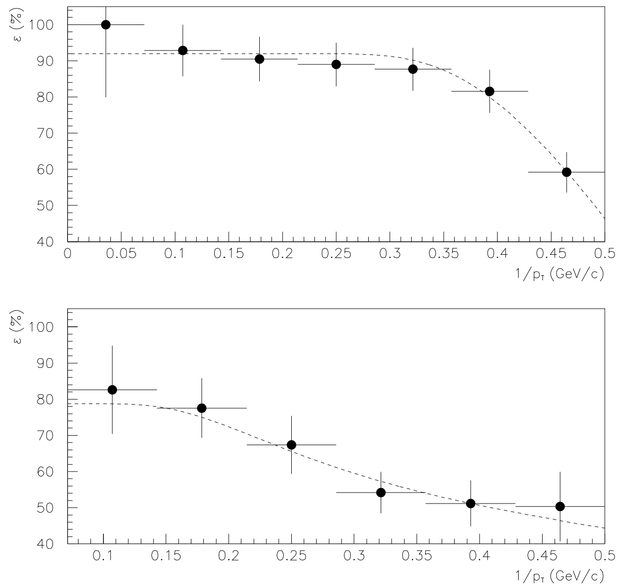

Figure 15: *Run II Level 2 low p_T muon trigger efficiency in terms of $1/p_T$ threshold (top for* CMU *and bottom for* CMX*).*

Before studying the Level 2 efficiency, it is worthwhile taking a look to the Level 1 Run I efficiency, shown in fig. 14; this offers two pieces of information: first, it allows a cross-check of the unbiased sample by means of a comparison with the results obtained in [11] (indicated by the dotted curves in figure). Secondly, it shows that the the Run I Level 1 low p_T trigger requirement is characterized by a smooth turn-up at low p_T: a significant efficiency level ($\gtrsim 70\%$ for CMU and $\gtrsim 50\%$ for CMX) is preserved even below the nominal threshold of 3.3 GeV/c, which reduces the RUN2TRS sensibility from the Run I Level 1 muon requirement, allowing in this way to study the Run II trigger performances down to ~ 2 GeV/c, which represents some lower working limit for the XFT.

A graphical representation of the p_T dependence of ϵ_μ for Run II Level 2 requirement, on the other hand, is shown in fig. 15, where the dotted curves are fited to the experimental points according to the function[16] described on pag. 6 of [11].

The method for computing the probability of selecting 'signal' events[17] follows from the convolution procedure used for electrons, which led to the expression (3): the weight applied

[16] The function used, although being capable of representing the experimental data, is the result of a Level 1 (Run I) trigger model; the corresponding function for Level 2 depends strongly on a CFT modelling and, for this reason, has not been used.

[17] In this case events containing a muon fiducial in some muon chamber and which has been produced in the semileptonic decay of a B or D-hadron coming from V or H^0.

per muon[18] depends on its p_T according to fig. 15. The expression for the event efficiency therefore assume the more general form:

$$P_{evt} = 1 - \prod (1 - \epsilon_\mu(p_T)) \ , \tag{5}$$

where the product is extended over all signal muons of the event (each associated to a specific value of $\epsilon_\mu(p_T)$) which fall in some muon chamber fiducial volume.

A rescaling has been performed on data for estimating the effect of the increase in acceptance (of a factor ~ 1.5) of the CMX on Level 2 efficiencies and rates. In order to do this, the total rate has been written as the sum of two contributions:

$$\mathcal{R}ate(total) = \mathcal{R}ate(\text{CMU}, \text{CMU} + \text{CMX}) + \mathcal{R}ate(\text{CMX}) \ ,$$

where $\mathcal{R}ate(\text{CMU}, \text{CMU} + \text{CMX})$, being the contribution from events with at least one signal μ falling in the CMU acceptance, does not depend on the CMX geometry; therefore, assuming an azimuthally symmetric events, the increase in the CMX acceptance can be kept entirely described considering:

$$\mathcal{R}ate(\text{CMX}) \longrightarrow 1.449 \times \mathcal{R}ate(\text{CMX}) \ .$$

A different approach could be followed for computing the expected efficiency enhancement: in this case, the effect of the CMX acceptance increase can be read in terms of a redefinition of the track fiduciality in the CMX; in principle, this is easy to do once the detailed CMX geometry and the magnetic field in the return yoke traversed by tracks flying towards muon chambers are known. However, since this would still not take into account the simulation for the CMX extention (needed as a starting point for RUN2TRS), the same procedure used for the rate has been followed. In this way, at Level 2, the CMX extended acceptance induces an enhancement of $\sim 15\%$ on the rate and $\sim 30\%$ on the efficiency respectively.

At this point, the Level 2 muon requirements have been studied in terms of their efficiency and rate for different values of the μ p_T and $\Sigma E_T 10$; while contributions to the efficiency have been discussed above, contributions to the rate comes from those background events which contain at least one XFT track passing the p_T requirement and that can be associated to a muon stub in the CMU or in the CMX.

[18]Here a XFT track associated to a TRKS track with CMU or CMX information.

As shown in fig. 16 and in table 2, muon-based Level 2 requirements on their own would be perfectly admissable, since the efficiency drop induced by muon acceptance[19] is balanced by a more consistent rate rejection. Nevertheless, owing to the behaviour of the electron requests (see § 5.2.1), no lepton-oriented Level 2 requirements can be applied together with purely calorimetric requests. This means that this Level 2 trigger path will enter Level 3 with an efficiency of 77.6% and a rate of 15.4 Hz, which, as anticipated on pag. 5, is an acceptable value.

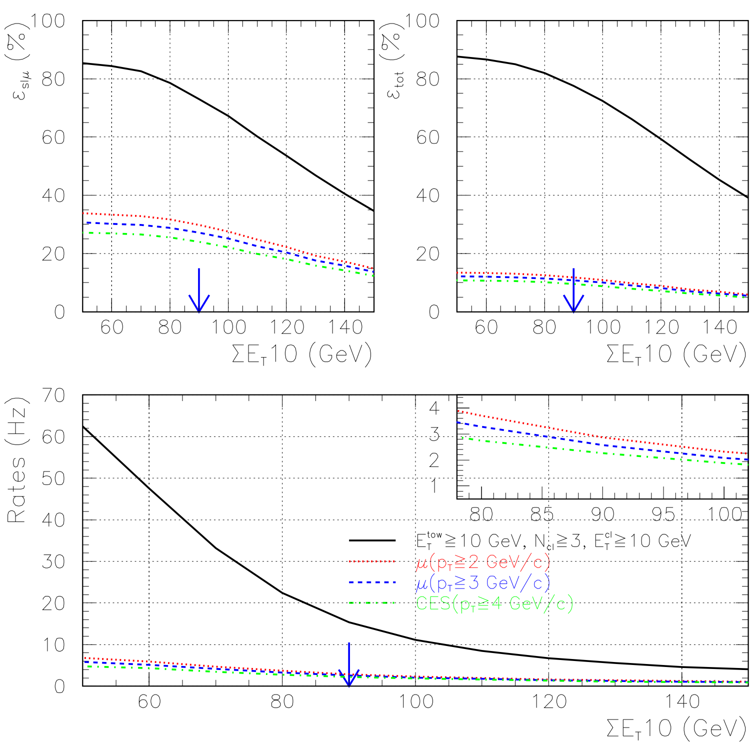

Figure 16: *Level 2 efficiency in events with at least one 'signal' muon (upper left), in* $H^0+Z^0/W^\pm \to$ *had events (upper right) and rate (below) in terms of* $\Sigma E_T 10$.

Selection	**Efficiency**	**Rate** (JET20)
Calorimetry only	73.0% (77.6%)	15.4 Hz
$p_T(\mu) \geqslant 2$ GeV/c	29.8% (11.8%)	2.87 Hz
$p_T(\mu) \geqslant 3$ GeV/c	27.1% (10.8%)	2.58 Hz
$p_T(\mu) \geqslant 4$ GeV/c	24.0% (9.53%)	2.26 Hz

Table 2: *Level 2 event efficiencies and rates for* $\Sigma E_T 10 \geqslant 90$ GeV *(efficiencies are computed with respect to the total number of events in which a signal muon has been produced – efficiencies on* $H^0+Z^0/W^\pm \to$ *had are indicated in brackets).*

[19] The fraction of events in which a signal muon has been produced within CMU or CMX acceptance ranges between 29.6 and 22.9% according to the P_T cut after calorimetric requirements ($\Sigma E_T 10 \geqslant 90$ GeV).

6 Level 3

The guiding idea for the Level 3
selection is the combination of calorimetric and lepton primitives; as shown in the previous section (in particular § 5.2.1), this procedure is not possible at Level 2, where the trigger requirements are purely calorimetric.

6.1 Calorimetry

At Level 3, calorimetry requirements essentially are aimed at confirming the Level 2 requirements; this, in particular, means that events passing the Level 3 should have at least 3 jets[20] with a minimum transverse energy content of 10 GeV. Similarly, there will be a requirement on ΣE_T^{jet}, but the value of the cut will be decided after the lepton requirements in order to keep control of the rate.

6.2 Soft Lepton Tag

Lepton requirements follow directly from the Soft Lepton Tag (SLT) algorithm developed during Run I for the top analysis and whose details are described elsewhere (see [12] for a complete review). The SLT is based on a two-fold procedure, designed to work differently on data and Monte Carlo; while data are treated applying the specific selections that will be recalled in the following sections (see § 6.2.1 and 6.2.2), the Monte Carlo procedure identifies all signal leptons[21] produced in the event and that are within detector acceptance, associating each of them to a tagging efficiency which has been estimated on true leptons collected from suitable datasets. The Monte Carlo procedure has been modified with respect to the original SLT version in order to adapt it to the considered signal.

Since the SLT requirements were optimized for the top search, we have checked the variables that could be affected by the different signal topology.

6.2.1 Electron tag

The electron selection is based on matching a track[22] with $p_T \geqslant 2\,\mathrm{GeV/c}$ with calorimetric quantities, tipically energy depositions in the CEM, CES and CPR detectors; at the same

[20] Jets cone $r_{\eta\phi} = 0.4$

[21] Again, here a signal lepton is a lepton produced in the semileptonic decay of a B or D-hadron coming from a boson.

[22] Here a fully reconstructed TRKS track fulfilling standard quality criteria and fiducial requirements – i.e. extrapolating in the instrumented region of the CEM detector ($|\eta| \lesssim 1$).

time, the quality of this matching has been taken into account by comparing the p_T and the extrapolated position of the track at the CES detector respectively with its e.m. tranverse energy deposition in the CEM calorimeter and the position of the matched cluster in the CES[23].

Soft electron requirements can be broadly divided into two classes according to their isolation dependence; in this way[24]:

- $|\Delta x_{CES}| \leqslant \max\{0.7\,\mathrm{cm}, 1.82\,\mathrm{cm} - 0.1867 \times \mathrm{p}\}$
- $|\Delta z_{CES}| \leqslant 2\,\mathrm{cm}$
- $E_{s_5}/p,\, E_{w_5}/p \geqslant \begin{cases} 0.24 + 0.03 \times p & \text{if } p \leqslant 12\,\mathrm{GeV/c} \\ 0.6 & \text{if } p > 12\,\mathrm{GeV/c} \end{cases}$
- $\chi^2_{strip}/6, \chi^2_{wire}/6 \leqslant 16$
- $Q_{CPR} \geqslant 4744 - 11592 \times (p/p_T) + 7923 \times (p/p_T)^2$

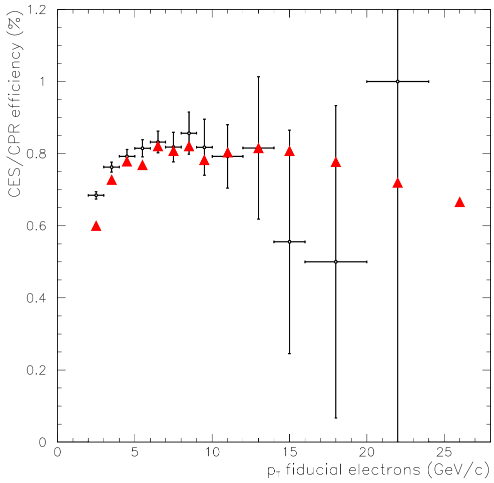

Figure 17: CES *and* CPR *combined efficiency as a function of track* p_T *for conversion electrons.*

belong to the isolation-independent class, since the soft electron variables in terms of which they are defined do not depend onto the track isolation. Therefore, their efficiency can be safely estimated from real data by means of a suitable sample of unbiased electrons (see crosses in fig. 17): for the purpose of cross-checking the efficiency quoted in [12] (triangles in fig. 17), the same conversion sample defined for Level 2 studies (see pag. 7) has been used. Looking at fig. 17, an efficiency enhancement has been observed at low p_T with respect to the standard SLT measurement; this is probably due to a higher purity of the conversion sample achieved by tagging the leading leg of each conversion by means of a trigger which requires XCES information[25]. At the same time, in order to avoid the trigger bias, it has been necessary to remove from the unbiased sample all electrons extrapolating to a CEM tower already matched to a trigger electron. Furthermore, fig. 17 shows that conversion electrons do represent a dangerous source of background and that, therefore, a conversion veto[26] has to be included in the selection.

[23] A cluster in the CES detector is considered only if its wire and strip profiles are compatible with an electron cluster hypothesis.

[24] Expressing energies in GeV and p, p_T in GeV/c; Q_{CPR} is expressed in terms of ADC counts.

[25] The trigger used for selecting the unbiased electron sample is CEM_8_CFT_7_5_XCES, while CEM_8_CFT_7_5 has been used in [12].

[26] Whose details are described in [12].

On the other hand, considering the class of isolation-dependent quantities, the requirements:

- $0.7 \leqslant E_{em}/p \leqslant 1.5$
- $E_{had}/E_{em} \leqslant \begin{cases} 0.1 & \text{if } \textit{flat } E_{em}/p \text{ cut} \\ 0.05 + \sum_p^{0.2} / E_{em} & \text{if } \textit{sliding } E_{em}/p \text{ cut} \end{cases}$

need to be studied on the signal Monte Carlo in order to keep into account the intrinsic dependence on the environment track density of the variables they are applied on. However, as a cross-reference, these quantities have been studied on the unbiased conversion electron sample as well (see fig. 18 for E_{em}/p and fig. 19 for E_{had}/E_{em}), without evidentiating remarkable discrepancies with respect to the Monte Carlo.

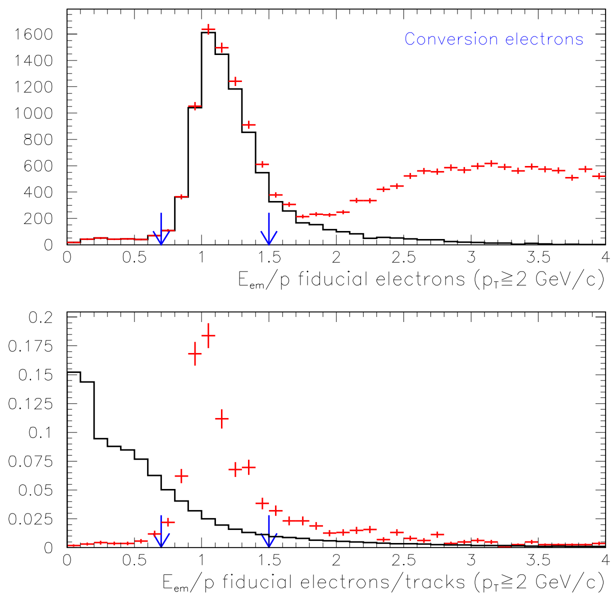

Figure 18: *Top: E_{em}/p for conversion electrons (crosses: all conversion soft legs; solid: conversion soft legs extrapolating to a* CEM *tower matched to a trigger electron have been removed). Bottom: E_{em}/p for signal Monte Carlo (crosses) and background (solid).*

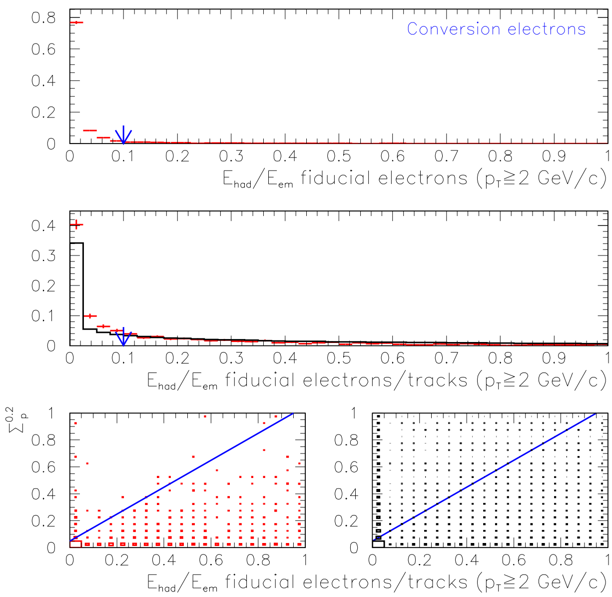

Figure 19: *Top: E_{had}/E_{em} (flat) for conversion electrons. Middle: E_{had}/E_{em} (flat) for signal Monte Carlo. Bottom: E_{had}/E_{em} vs. $\sum_p^{0.2}$ for for signal Monte Carlo (left) and background (right).*

The standard SLT algorithm includes also a cut on the dE/dx (see [12]); in this context, however, this request has been kept separated from the others, since its isolation-dependence is still under study. Furthermore, stable calibrations are not yet available at Level 3.

The procedure for computing the event tagging probability[27]; is formally identical to the one used at Level 2 for the electron selection, four different possible alternatives have been examined, as a result of switching between the *flat* or *sliding* E_{had}/E_{em} cut and of turning on or off the dE/dx requirement. Efficiencies and rate behaviours have then been monitored in function of ΣE_T^{jet} and the results summarized in fig. 20.

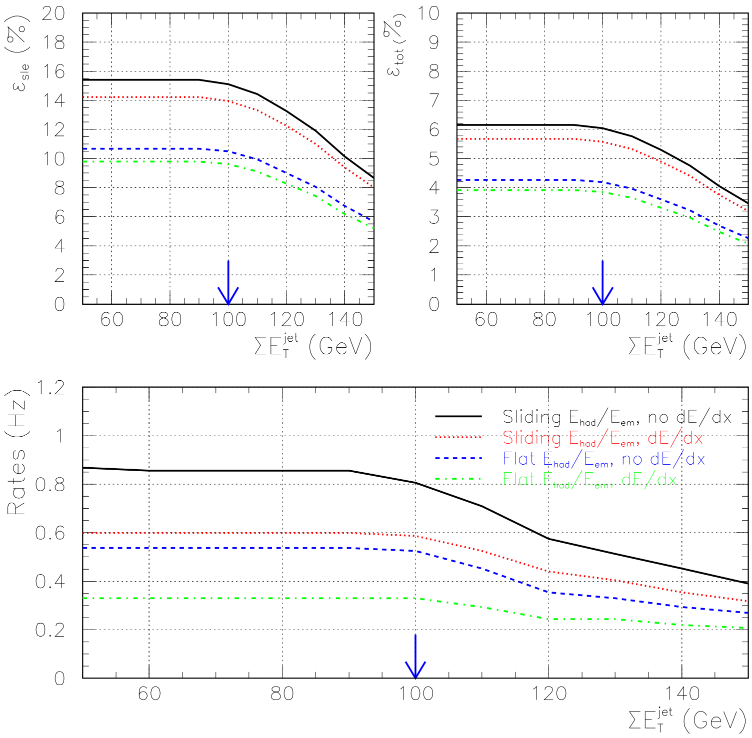

Figure 20: *Level 3 efficiency in events with at least one 'signal' electron (upper left), in* $H^0+Z^0/W^\pm \to$ *had events (upper right) and rate (below) in terms of* ΣE_T^{jet}.

6.2.2 Muon tag

At Level 3, the selection criteria follow directly from the SLT algorithm requirements; therefore, tracks[28], which are required to have $p_T \geqslant 2\,\mathrm{GeV/c}$, are divided into four classes according to the muon detectors they extrapolate to (see [12]):

- CMUP: the track extrapolates within the fiducial volumes of both CMU and CMP
- CMP: the track extrapolates within the CMP fiducial volume and is not CMU-fiducial
- CMU: the track extrapolates within the CMU fiducial volume and is not CMP-fiducial
- CMX: the track extrapolates within the CMX fiducial volume

[27] SLT electron tagging efficiencies (i.e. the 'triangles' of fig. 17) have been used.
[28] As in the case of electrons, fully reconstructed TRKS tracks fulfilling standard quality requests are considered.

Once the track fiduciality has been defined, a track–stub matching procedure is performed, where essentially a stub is required for each detector the track is fiducial within; then, most of the muon requirements relate to the track–stub match that has been so far established[29]. Furthermore, the minimum ionizing requirement:

- $E_{had} - \sum_p^{0.2} < 6\,\mathrm{GeV/c}$

has been asked for all muon candidates with $p_T > 6\,\mathrm{GeV/c}$.

The increase in acceptance of the CMX has been treated as in the case of Level 2 (see pag. 15); in the case of Level 3, this induces an enhancement of $\sim 30\%$ on the efficiency, while the effect on the rate is negligible. As in the case of electrons, the standard SLT values for soft muon tagging have been used for computing the event tagging probabilities[30]. The results, in function of ΣE_T^{jet}, are shown in fig. 21.

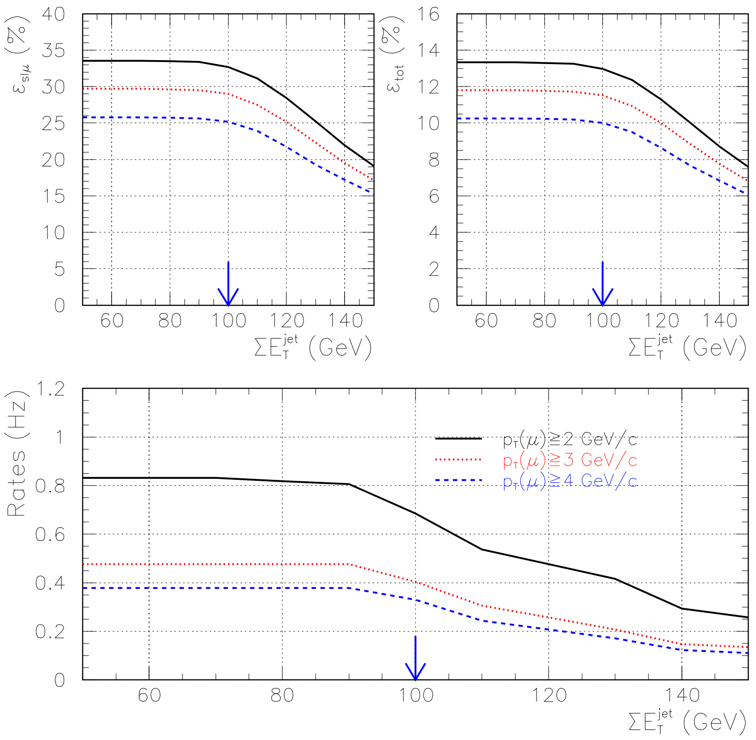

Figure 21: *Level 3 efficiency in events with at least one 'signal' muon (upper left), in* $H^0 + Z^0/W^\pm \to$ *had events (upper right) and rate (below) in terms of* ΣE_T^{jet}.

6.3 Combined SLT

Once the soft lepton tagging procedure has been tested separately for electrons and muons, a combined strategy has to be defined for the Level 3 selection; at this point, when all possible primitives have already been defined (and, with them, their efficiency), the main problem is keeping the rate at an acceptable value ($\sim 1\,\mathrm{Hz}$).

[29] Refer to [12] for details.

[30] Same procedure used previously for Level 2 and in the case of electrons.

In fig. 22, which has been obtained combining the two most efficient lepton requests (*sliding* E_{had}/E_{em} cut and no $\mathrm{d}E/\mathrm{d}x$ requirement for electrons and $p_T(\mu) \geqslant 2\,\mathrm{GeV/c}$ for muons) with all calorimetric requirements[31], the efficiency and rate behaviours are shown in terms of the cut value for ΣE_T^{jet}, which, at this point, represents the only 'free parameter' we can act on to reduce the rate.

The considered combination of single lepton primitives is acceptable in terms of rate for $\Sigma E_T^{jet} \geqslant 100\,\mathrm{GeV}$; for this situation, values for the efficiencies and the rate are reported in table 3.

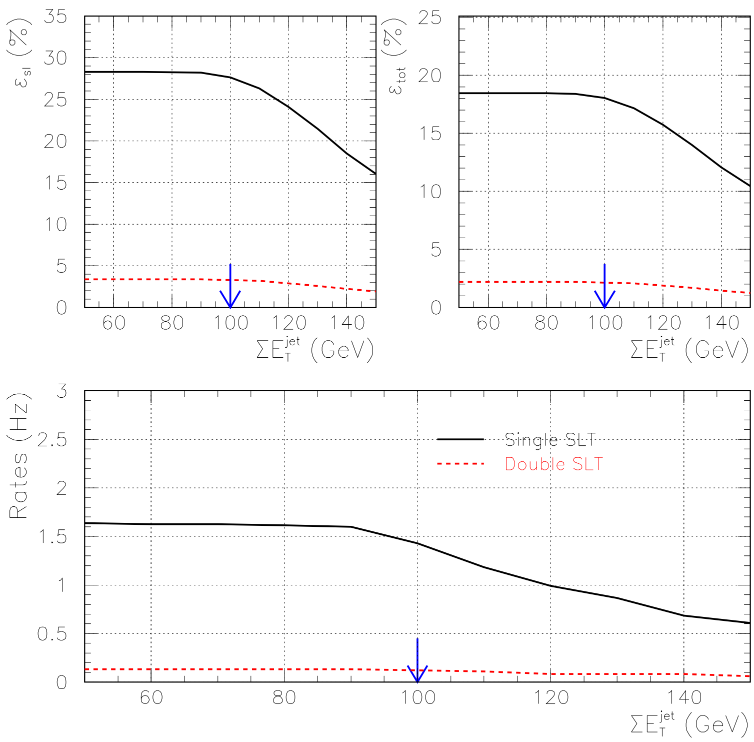

Figure 22: *Level 3 efficiency in events with at least one 'signal' lepton (upper left), in* $\mathrm{H^0{+}Z^0/W^{\pm}} \rightarrow$ *had events (upper right) and rate (below) in terms of* ΣE_T^{jet}.

Selection	Efficiency	Rate (JET20)
Single SLT	27.6% (18.0%)	1.43 Hz
Double SLT	3.30% (2.15%)	0.122 Hz

Table 3: *Level 3 efficiencies and rates for* $\Sigma E_T^{jet} \geqslant 100\,\mathrm{GeV}$ *for two different* SLT *requests (efficiencies are computed with respect to the total number of events in which a signal muon has been produced – efficiencies on* $\mathrm{H^0{+}Z^0/W^{\pm}} \rightarrow$ *had are indicated in brackets). Level 1, 2 and 3 calorimetric requirements are included.*

[31] Level 1, Level 2 and Level 3 (see § 6.1) requests.

7 Proposal

In this note we present the proposal for a multijet trigger for (SM) Higgs associated production with a vector boson, especially aimed at tagging the leptons produced in the semileptonic decays of their B and D-hadrons.

The essential requirements which have been proposed for this trigger are:

LEVEL 1: single trigger-tower $E_T^{tow} \geqslant 10\,\mathrm{GeV}$

LEVEL 2: $\Sigma E_T 10 \geqslant 90\,\mathrm{GeV}$, $N_{cl} \geqslant 3$ ($E_T^{cl} \geqslant 10\,\mathrm{GeV}$)

LEVEL 3: $\Sigma E_T^{jet} \geqslant 100\,\mathrm{GeV}$, $N_{jet}^{0.4} \geqslant 3$ ($E_T^{jet} \geqslant 10\,\mathrm{GeV}$), soft electron OR mu tag

The total efficiency, including the effects due to the increased CMX acceptance in Run II, is 18.0%, corresponding to a rate of 1.43 Hz. The efficiency value obtained on a $\mathrm{H}^0\mathrm{V}$ signal (a 15.3% is estimated when the CMX upgrade is not taken into account) is therefore comparable to the result achieved by the SLT algorithm[32] on a ℓ+*jets* $\mathrm{t\bar{t}}$ signal with similar jet multiplicity (15.6%, see [13]).

The obtained results refer to a situation where a full track reconstruction scenario has been assumed at Level 3; further investigations, aimed at considering a less sophisticated event reconstruction at Level 3 – such as regional reconstruction –, as well as at monitoring the trigger dependencies from instantaneous luminosity, are in progress. As a second step, this work will move into the Run II framework, which will give also the opportunity of studying efficiency and rate contributions due to the increased η-tracking capability.

References

[1] Higgs Working Group, **Report of the Higgs Working Group**, Mar 2000

[2] J. Benlloch, W. Bokhari, J. Friedman, L. Rosenson, P. Sphicas, **The multijet data sample**, CDF internal note 2916, Dec 1994.

[3] P. Azzi, W. Bokhari, A. Castro, P. Sphicas, **Combined $\mathrm{t\bar{t}}$ production cross section in the fully hadronic final state**, CDF internal note 3767, Jul 1996.

[4] J. Troconiz, R. Vilar, J. Valls, **Search for Higgs Bosons Produced in Association with a Vector Boson in $\mathrm{p\bar{p}}$ Collisions at 1.8 TeV**, Phys. Rev. Lett. **81**, 5748 (1998).

[32] In the $\mathrm{t\bar{t}}$ case, the E_{had}/E_{em} *flat* cut has been used.

[5] The Trigger and Datasets Working Group, **Run-II Trigger Table and Datasets Plan**, CDF internal note 4718, in preparation.

[6] J. Troconiz, J. A. Valls, R. Vilar, **Update in the Search for a Neutral Heavy Scalar in the Multijet Data Sample**, CDF internal note 4129, Nov 1997.

[7] The CDF II Collaboration, **The CDF II Detector Technical Design Report**, FERMILAB-PUB-96-390-E, Oct 1996.

[8] K. Byrum, A. B. Wicklund, **E_T Dependence of the XCES Trigger**, CDF internal note 4424, Nov 1997.

[9] T. Asakawa, S. Geer, **Further Properties of High-Mass Multijet Events at the Fermilab Proton-Antiproton Collider**, Phys. Rev. Lett. **75**, 608 (1995).

[10] M. Tanaka, Private Communication.

[11] S. P. Pappas *et al.*, **Run 1B Low p_T Central Dimuon Trigger Efficiencies**, CDF internal note 4076, Feb 1997.

[12] C. Campagnari, D. Kestenbaum, **Review of the SLT Algorithm for Run 1b**, CDF internal note 3682, May 1996.

[13] G. Apollinari *et al.*, **Measurement of the $t\bar{t}$ production cross section using SLT tags.**, CDF internal note 3861, Nov 1996.